Articles

Synthesis of Helical Poly(*N*-propargylamides) Carrying Azobenzene Moieties in Side Chains. Reversible Arrangement-Disarrangement of Helical Side Chain Arrays upon Photoirradiation Keeping Helical Main Chain Intact

Toru Fujii,[†] Masashi Shiotsuki,[†] Yoshihito Inai,[‡] Fumio Sanda,*[,†] and Toshio Masuda*[,†]

Department of Polymer Chemistry, Graduate School of Engineering, Kyoto University, Katsura Campus, Kyoto 615-8510, Japan, and Department of Environmental Technology and Urban Planning, Shikumi College, Graduate School of Engineering, Nagoya Institute of Technology, Gokiso-cho, Showa-ku, Nagoya 466-8555, Japan

Received April 19, 2007; Revised Manuscript Received July 18, 2007

ABSTRACT: Optically active novel *N*-propargylamides bearing azobenzene, (*R*)-HC≡$CCH_2NHCOCH(CH_3)$O-1,4-C_6H_4−N═N−C_6H_5 (**1a**), (*R*)-HC≡$CCH_2NHCOCH(CH_3)$O-1,4-C_6H_4−N═N-1′,4′-C_6H_4-*n*-hexyl (**1b**), (*R*)-HC≡$CCH_2NHCOCH(CH_2C_6H_5)$O-1,4-C_6H_4−N═N−C_6H_5 (**2a**), (*R*)-HC≡$CCH_2NHCOCH(CH_2C_6H_5)$O-1,4-C_6H_4−N═N-1′,4′-C_6H_4-*n*-hexyl (**2b**), and (*R*)-HC≡$CCH_2NHCOCH(C_6H_5)$O-1,4-C_6H_4−N═N−C_6H_5 (**3**) were synthesized and polymerized with $[(nbd)RhCl]_2$ as a catalyst to obtain the corresponding polymers with moderate molecular weights (M_n = 6900−44 000) in 46−99% yields. Polarimetric, CD, UV−vis, NOE−NMR, and IR spectroscopic studies demonstrated that the resulting polymers took a helical structure with predominantly one-handed screw sense stabilized by intramolecular hydrogen bonding between the amide groups in the side chains in various solvents. The CD spectra simulated by molecular orbital calculation well agreed with the experimental ones, and indicated the arrangement of azobenzene moieties in a mutual chiral geometry of one-handed screw sense. The *trans*-azobenzene in the side chain isomerized into the *cis* form upon UV irradiation, while the helical structure of the main chain was not affected so much. The *cis*-azobenzene reisomerized into the *trans* form upon visible-light irradiation, which induced a recovery of chiral geometry of azobenzene moieties in the side chain. Poly(**1b**) formed a cholesteric liquid crystal.

Introduction

Azobenzene is a typical photoresponsive chromophore that undergoes reversible photoisomerization between *trans* and *cis* forms.[1] Polymers carrying azobenzene moieties including polypeptides,[2] polyisocyanates,[3] polymethacrylates,[4] polysilanes,[5] polyisocyanides,[6] and polyketones[7] are of great interest not only because of the change of optical properties but also because of the potential application to optical memories and liquid crystalline materials.[8]

Substituted polyacetylenes have unique properties such as high gas permeability, nonlinear optical properties, formation of ferroelectric liquid crystals and helical structures.[9] Monosubstituted acetylenes undergo polymerization with Rh catalysts to give the corresponding polyacetylenes with stereoregular *cis* structure.[10] When the substituents are appropriately bulky, they form a helical structure due to the rigid main chain.[11] Poly(*N*-propargylamides),[12] poly(*N*-propargylcarbamates),[13] and poly(propargyl esters)[14] carrying amide or hydroxy groups form a helical structure stabilized by intramolecular hydrogen bonding as well as steric repulsion between the side chains, some of which undergo reversible helix−helix or helix−coil transition upon temperature and solvent changes.

We have previously reported the synthesis and properties of helical poly(*N*-propargylamides) bearing azobenzene moieties in the side chain.[15] The azobenzene moieties reversibly isomerize between *cis* and *trans* forms upon photoirradiation. However, once the helical polymers have transformed into random coil structure in conjunction with the isomerization of the azobenzne moieties upon UV-light irradiation, they do not recover the original helicity upon visible-light irradiation. Further molecular design is necessary to achieve reversible transformation of higher order structures triggered by azobenzene isomerization. In the course of our study aiming at such kind of reversible systems, we have unexpectedly found a very unique system that shows reversible arrangement−disarrangement of helical side chain arrays upon photoirradiation, keeping the helical main chain intact. The present study deals with synthesis of chiral poly(*N*-propargylamides) carrying azobenzene moieties (Scheme 1), and reversible transformation of secondary structure upon photoirradiation. It also discloses the responsiveness of the polymers to heat and solvent, along with liquid crystalline properties.

* Corresponding authors. E-mail: (F.S.) sanda@adv.polym.kyoto-u.ac.jp; (T.M.) masuda@adv.polym.kyoto-u.ac.jp.
[†] Kyoto University.
[‡] Nagoya Institute of Technology.

10.1021/ma070917j CCC: $37.00
Published on Web 09/05/2007

Scheme 1. Polymerization of 1a−3

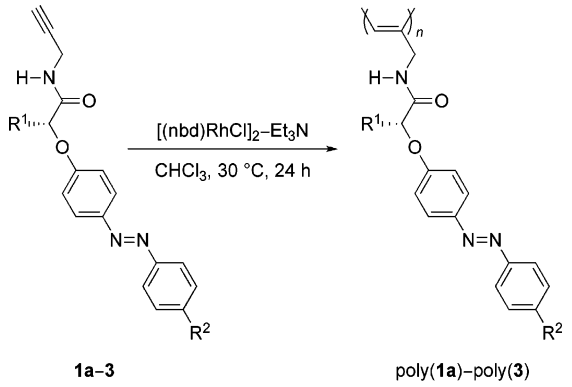

1a–3 poly(**1a**)–poly(**3**)

1a: $R^1 = CH_3$, $R^2 = H$, **1b**: $R^1 = CH_3$, $R^2 = C_6H_{13}$
2a: $R^1 = CH_2C_6H_5$, $R^2 = H$, **2b**: $R^1 = CH_2C_6H_5$, $R^2 = C_6H_{13}$
3: $R^1 = C_6H_5$, $R^2 = H$

Experimental Section

Measurements. Melting points (mp) were measured on a Yanaco micromelting point apparatus. Specific rotations ($[\alpha]_D$) were measured by a JASCO DIP-1000 digital polarimeter. IR spectra were obtained with a JASCO FTIR-4100 spectrophotometer. NMR (^{1}H, 400 MHz; ^{13}C, 100 MHz) spectra were recorded on a JEOL EX-400 spectrometer. Elemental analyses were conducted on Yanaco CHN Corders MT-2, -3, -5, and -6 at the Kyoto University Elemental Analysis Center. Number-average molecular weights (M_n) and molecular weight distributions (M_w/M_n) of polymers were estimated by GPC (Shodex KF-850L columns) eluted with $CHCl_3$ by polystyrene calibration. Viscosity indices were determined by GPC equipped with viscometer and right-angle laser light scattering detectors (Viscotek T60A) eluted with THF at 40 °C. CD and UV−vis spectra were recorded on a JASCO J-820 spectropolarimeter. Unless otherwise specified, UV−vis and CD spectra of polymers were measured at a concentration of 0.10 mM based on the monomer unit at 20 °C. Polarized optical microscope images were captured with a Nikon ECLIPSE LV100POL.

Materials. Propargylamine (Aldrich), L-(+)-lactic acid (Wako), L-(−)-3-phenyllactic acid (Aldrich), (*S*)-(+)-mandelic acid (Wako), 4-hydroxyazobenzene (Wako), 4-octylphenol (Wako), and 4-(4,6-dimethoxy-1,3,5-triazin-2-yl)-4-methylmorpholinium chloride (TRIAZIMOCH, Tokuyama) were used as received. Methyl (*S*)-(−)-lactate,[16] 4-(4-hexylphenylazo)phenol,[17] and $[(nbd)RhCl]_2$[18] were prepared according to the literature. The $CHCl_3$ used for polymerization was distilled before use.

Synthesis of (*R*)-2-(4-Phenylazophenoxy)-*N*-propargylpropionamide (1a). A solution of diisopropyl azodicarboxylate (40% in toluene, 2.02 mL, 10.0 mmol) in anhydrous THF (15 mL) was added to a solution of methyl (*S*)-(−)-lactate (1.04 g, 10.0 mmol), 4-hydroxyazobenzene (1.98 g, 10.0 mmol), and triphenylphosphine (2.62 g, 10.0 mmol) in anhydrous THF (40 mL) dropwise at 0 °C under nitrogen atmosphere, and the resulting mixture was stirred at room temperature for 2 days. The precipitated solid (triphenylphosphine oxide) was filtered off, then the filtrate was concentrated on a rotary evaporator, and the residual mass was purified by silica gel column chromatography eluted with hexane/ethyl acetate to obtain (*R*)-2-(4-phenylazophenoxy)propionic acid methyl ester (0.650 g, 2.29 mmol, yield 23%). To a solution of (*R*)-2-(4-phenylazophenoxy)propionic acid methyl ester (0.650 g, 2.29 mmol) in MeOH, 1 M NaOH aqueous solution (2.29 mL, 2.29 mmol) was added at 0 °C, and the resulting mixture was stirred at 0 °C for 30 min. The reaction mixture was concentrated with a rotary evaporator and acidified with 2 M HCl. $CHCl_3$ (ca. 100 mL) was added to the mixture, and the resulting solution was extracted with $CHCl_3$. The organic layer was washed with 2 M HCl and a saturated aqueous NaCl, dried over $MgSO_4$, and concentrated to obtain a mixture of (*R*)-2-(4-phenylazophenoxy)propionic acid and (*R*)-2-(4-phenylazophenoxy)propionic acid methyl ester (75/15). This mixture containing (*R*)-2-(4-phenylazophenoxy)propionic acid (0.500 g, 1.85 mmol) was added to a solution of propargylamine (0.100 g, 1.85 mmol) and TRIAZIMOCH (15 wt % H_2O, 0.600 g, 1.85 mmol) in THF (100 mL), and the resulting mixture was stirred at room temperature overnight. After white precipitate was filtered off, the filtrate was concentrated with a rotary evaporator. $CHCl_3$ (ca. 100 mL) was added to the residue, and the resulting solution was washed with 2 M HCl and saturated aqueous $NaHCO_3$, dried over anhydrous $MgSO_4$, and concentrated. Then, the residue was dried under reduced pressure, and purified by silica gel column chromatography eluted with hexane/ethyl acetate (4/1−2/1, volume ratio) to obtain monomer **1a** (0.400 g, 1.30 mmol, yield 57%). Mp: 130.6−131.0 °C. $[\alpha]_D = +68$ deg ($c = 0.10$ g/dL in $CHCl_3$). IR ($CHCl_3$): 3441 (ν_{N-H}), 3309 ($\nu_{H-C\equiv}$), 3019, 2117 ($\nu_{C\equiv C}$), 1682 ($\nu_{C=O}$), 1520 (δ_{N-H}), 1214 (ν_{C-O}), 736, 669 cm^{-1}. ^{1}H NMR ($CDCl_3$): δ 1.61 (C*H*$_3$, d, $J = 6.8$ Hz, 3H), 2.21 (C≡C*H*, t, $J = 2.4$ Hz, 1H), 4.00−4.15 (C≡CC*H*$_2$, m, 2H), 4.79 (C*H*, q, $J = 6.8$ Hz, 1H), 6.61 (N*H*, s, 1H), 7.00−7.03 (Ar*H*, m, 2H), 7.42−7.51 (Ar*H*, m, 3H), 7.85−7.93 (Ar*H*, m, 4H). ^{13}C NMR ($CDCl_3$): δ 18.5, 28.9, 71.89, 75.09, 78.88, 115.71, 122.66, 124.87, 129.06, 130.70, 147.85, 152.61, 158.86, 171.33. Anal. Calcd for $C_{18}H_{17}N_3O_2$: C, 70.34; H, 5.58; N, 13.67. Found: C, 70.16; H, 5.72; N, 13.56.

Synthesis of (*R*)-2-[4-(4-Hexylphenylazo)phenoxy]-*N*-propargylpropionamide (1b). Monomer **1b** was synthesized from methyl (*S*)-(−)-lactate and 4-(4-hexylphenylazo)phenol in a manner similar to monomer **1a**. Yield from methyl (*S*)-(−)-lactate: 8.9%. Mp: 125.4−126.0 °C. $[\alpha]_D = +52$ deg ($c = 0.10$ g/dL in $CHCl_3$). IR ($CHCl_3$): 3435 (ν_{N-H}), 3309 ($\nu_{H-C\equiv}$), 3019, 2117 ($\nu_{C\equiv C}$), 1682 ($\nu_{C=O}$), 1520 (δ_{N-H}), 1212 (ν_{C-O}), 740, 669 cm^{-1}. ^{1}H NMR ($CDCl_3$): δ 0.87 ($CH_2CH_2CH_2CH_2CH_2CH_3$, t, $J = 6.8$ Hz, 3H), 1.30 ($CH_2CH_2CH_2CH_2CH_2CH_3$, broad s, 6H), 1.56−1.65 (C*H*$_3$, $CH_2CH_2CH_2CH_2CH_2CH_3$, m, 5H) 2.21 (C≡C*H*, t, $J = 2.4$ Hz, 1H), 2.66 ($CH_2CH_2CH_2CH_2CH_2CH_3$, t, $J = 7.6$ Hz, 2H), 4.06−4.15 (C≡CC*H*$_2$, m, 2H), 4.78 (C*H*, q, $J = 6.8$ Hz, 1H), 6.61 (N*H*, s, 1H), 7.00 (Ar*H*, d, $J = 8.8$ Hz, 2H), 7.29 (Ar*H*, d, $J = 9.2$ Hz, 2H), 7.82 (Ar*H*, d, $J = 13.2$ Hz, 2H), 7.88 (Ar*H*, d, $J = 8.8$ Hz, 2H). ^{13}C NMR ($CDCl_3$): δ 14.07, 18.52, 22.59, 28.90, 28.93, 31.26, 31.69, 35.87, 71.88, 75.10, 78.90, 115.70, 122.65, 124.69, 129.08, 146.29, 147.96, 150.87, 158.63, 171. Anal. Calcd for $C_{24}H_{29}N_3O_2$: C, 73.63; H, 7.47; N, 10.73. Found: C, 73.46; H, 7.45; N, 10.65.

Synthesis of (*R*)-3-Phenyl-2-(4-phenylazophenoxy)-*N*-propargylpropionamide (2a). A solution of propargylamine (0.990 g, 18.1 mmol) and TRIAZIMOCH (15 wt % H_2O, 5.89 g, 18.1 mmol) in THF (200 mL) was added to a solution of L-(−)-3-phenyllactic acid (3.00 g, 18.1 mmol) at room temperature. The resulting mixture was stirred at room temperature overnight. White precipitate formed was filtered off, and the filtrate was concentrated with a rotary evaporator. $CHCl_3$ (ca. 100 mL) was added to the residue, and the resulting solution was washed with 2 M HCl and saturated aqueous $NaHCO_3$, dried over $MgSO_4$, and concentrated. Then, the residue was dried under reduced pressure, and the residual mass was purified by silica gel column chromatography eluted with hexane/ethyl acetate to obtain (*S*)-2-hydroxy-3-phenyl-*N*-propargylpropionamide (2.58 g, 12.7 mmol, yield 70.2%). A solution of diisopropyl azodicarboxylate (40% in toluene, 2.02 g, 10.0 mmol) in anhydrous THF (15 mL) was added to a solution of (*S*)-2-hydroxy-3-phenyl-*N*-propargylpropionamide (2.04 g, 10.0 mmol), 4-hydroxyazobenzene (1.88 g, 10.0 mmol), and triphenylphosphine (2.62 g, 10.0 mmol) in anhydrous THF (40 mL) dropwise under nitrogen atmosphere at 0 °C, and the resulting mixture was stirred at room temperature for 2 days. The precipitated solid (triphenylphosphine oxide) was filtered off, then the filtrate was concentrated with a rotary evaporator, and the residual mass was purified by silica gel column chromatography eluted with hexane/ethyl acetate to obtain monomer **2a** (0.36 g, 0.93 mmol, yield 19%). Mp: 130.6−131.0 °C. $[\alpha]_D = +5.3$ deg ($c = 0.10$ g/dL in $CHCl_3$). IR ($CHCl_3$): 3435 (ν_{N-H}), 3308 ($\nu_{H-C\equiv}$), 2931, 2153 ($\nu_{C\equiv C}$), 1681 ($\nu_{C=O}$), 1520 (δ_{N-H}), 1213 (ν_{C-O}), 740, 668 cm^{-1}. ^{1}H NMR ($CDCl_3$): δ 2.18 (C≡C*H*, s, 1H), 3.21−3.26 (C*H*HC_6H_5, dd, $J = 14.0$, 6.8 Hz, 1H), 3.33−

3.37 (CH*H*C_6H_5, dd, J = 14.0, 4.0 Hz, 1H), 3.99−4.04 (C≡CC*H*$_2$, m, 2H), 4.91−4.93 (C*H*, dd, J = 6.8 Hz, 4.0 Hz, 1H), 6.40 (N*H*, s, 1H), 6.94 (Ar*H*, d, J = 8.8 Hz, 2H), 7.22−7.30 (Ar*H*, m, 5H), 7.43−7.52 (Ar*H*, m, 3H), 7.86−7.89 (Ar*H*, m, 4H). ^{13}C NMR ($CDCl_3$): δ 28.82, 38.63, 71.81, 78.68, 79.65, 115.80, 122.66, 124.80, 126.97, 128.37, 129.06, 129.74, 130.70, 135.89, 147.89, 152.60, 159.16, 170.01. Anal. Calcd for $C_{24}H_{21}N_3O_2$: C, 75.18; H, 5.52; N, 10.96. Found: C, 74.51 H, 5.68; N, 10.98.

Synthesis of (*R*)-2-[4-(4-Hexylphenylazo)phenoxy]-3-phenyl-*N*-propargylpropionamide (2b). Except for using 4-(4-hexylphenylazo)phenol instead of 4-hydroxyazobenzene, **2b** was prepared in the same way as monomer **2a**. Yield from L-(−)-3-phenyllactic acid: 12.0%. Mp: 113.2−113.6 °C. $[\alpha]_D$ = −7.9 deg (c = 0.10 g/dL in $CHCl_3$). IR ($CHCl_3$): 3435 (ν_{N-H}), 3308 ($\nu_{H-C\equiv}$), 3011, 2200 ($\nu_{C\equiv C}$), 1682 ($\nu_{C=O}$), 1520 (δ_{N-H}), 1235 (ν_{C-O}) cm^{-1}. ^{1}H NMR ($CDCl_3$): δ 0.88 ($CH_2CH_2CH_2CH_2CH_2CH_3$, t, J = 6.8 Hz, 3H), 1.32 ($CH_2CH_2CH_2CH_2CH_2CH_3$, m, 6H), 1.63−1.66 ($CH_2CH_2CH_2CH_2CH_2CH_3$, m, 2H), 2.17 (C≡C*H*, s, 1H), 2.67 ($CH_2CH_2CH_2CH_2CH_2CH_3$, t, J = 7.6 Hz, 2H), 3.20−3.26 (C*H*C_6H_5, dd, J = 14.4, 6.8 Hz, 1H), 3.32−3.37 (CH*H*C_6H_5, dd, J = 14.4, 4.0 Hz, 1H), 4.00−4.03 (C≡CC*H*$_2$, m, 2H), 4.90−4.92 (C*H*, dd, J = 6.4 Hz, 3.6 Hz, 1H), 6.43 (N*H*, s, 1H), 6.95 (Ar*H*, d, J = 5.2 Hz, 2H), 7.23−7.31 (Ar*H*, m, 7H), 7.78−7.86 (Ar*H*, m, 4H). ^{13}C NMR ($CDCl_3$): δ 14.07, 22.57, 28.80, 28.91, 31.24, 31.67, 35.85, 38.61, 71.77, 78.69, 79.62, 115.78, 122.63, 124.60, 126.94, 128.35, 129.06, 129.73, 135.91, 146.28, 147.97, 150.84, 158.90, 170.06. Anal. Calcd for $C_{30}H_{33}N_3O_2$: C, 77.06; H, 7.11; N, 8.99. Found: C, 77.17; H, 7.15; N, 8.98.

Synthesis of (*R*)-2-[4-(4-Hexylphenylazo)phenoxy]-2-phenyl-*N*-propargylacetamide (3). Monomer **3** was synthesized from (*S*)-2-hydroxy-2-phenyl-*N*-propargylacetamide and 4-phenylazophenol in a manner similar to monomer **2a**. (*S*)-2-Hydroxy-2-phenyl-*N*-propargylacetamide was synthesized from (*S*)-(+)-mandelic acid and propargylamine. Yield from (*S*)-(+)-mandelic acid: 20%. Mp: 165.0−165.6 °C. $[\alpha]_D$ = −52 deg (c = 0.10 g/dL in $CHCl_3$). IR ($CHCl_3$): 3440 (ν_{N-H}), 3308 ($\nu_{H-C\equiv}$), 3019, 2200 ($\nu_{C\equiv C}$), 1685 ($\nu_{C=O}$), 1515 (δ_N-H), 1214 (ν_{C-O}) 738, 669 cm^{-1}. ^{1}H NMR ($CDCl_3$): δ 2.25 (C≡C*H*, s, 1H), 4.04−4.18 (C≡CC*H*$_2$, m, 2H), 5.66 (C*H*, t, J = 10.0 Hz, 1H), 6.90 (N*H*, s, 1H), 7.06 (Ar*H*, d, J = 14.4 Hz, 2H), 7.32−7.57 (Ar*H*, m, 8H), 7.87 (Ar*H*, t, J = 6.8 Hz, 4H). ^{13}C NMR ($CDCl_3$): δ 29.11, 72.07, 76.68, 78.83, 80.26, 116.12, 122.63, 124.74, 126.52, 128.82, 128.87, 129.04, 130.70, 135.53, 147.88, 152.58, 158.61, 168.84. Anal. Calcd for $C_{23}H_{19}N_3O_2$: C, 74.78; H, 5.18; N, 11.37. Found: C, 74.66; H, 5.32; N, 11.24.

Synthesis of (*R*)-2-[4-Octylphenoxy]-*N*-propargylpropionamide (4). Monomer **4** was synthesized in a manner similar to **2a**. Yield from L-(+)-lactic acid: 9.1%. Mp: 83.6−84.2 °C. $[\alpha]$ = +41 deg (c = 0.10 g/dL in $CHCl_3$). IR ($CHCl_3$): 3432 (ν_{N-H}), 3308 ($\nu_{H-C\equiv}$), 3018, 2930, 2200 ($\nu_{C\equiv C}$), 1677 ($\nu_{C=O}$), 1504 (δ_{N-H}), 1217 (ν_{C-O}) 738, 669 cm^{-1}. ^{1}H NMR ($CDCl_3$): δ 0.86 ($CH_2CH_2CH_2CH_2CH_2CH_2CH_3$, t, J = 6.4 Hz, 3H), 1.20−1.38 ($CH_2CH_2CH_2CH_2CH_2CH_2CH_2CH_3$, m, 8H), 1.38−1.48 ($CH_2CH_2CH_2CH_2CH_2CH_2CH_2CH_3$, br, 2H), 1.51 (*CH*$_3$, d, J = 6.8 Hz, 3H), 1.73 ($CH_2CH_2CH_2CH_2CH_2CH_2CH_2CH_3$, m, 2H), 2.20 (C≡C*H*, s, 1H), 3.88 ($CH_2CH_2CH_2CH_2CH_2CH_2CH_2CH_3$,t, J = 6.4 Hz, 2H), 4.00−4.13 (C≡CC*H*$_2$, m, 2H), 4.56 (*CH*, q, J = 12.8 Hz, 1H), 6.90 (N*H*, s, 1H), 6.80 (Ar*H*, br, 4H). ^{13}C NMR ($CDCl_3$): δ 14.09, 18.52, 22.62, 26.03, 28.81, 29.23, 29.31, 29.35, 31.80, 68.57, 71.72, 75.93, 75.09, 115.53, 116.95, 150.65, 154.45, 172.13. Anal. Calcd for $C_{20}H_{29}NO_3$: C, 72.47; H, 8.82; N, 4.23. Found: C, 72.03; H, 8.70; N, 4.00.

Polymerization Procedure. A $CHCl_3$ solution of a monomer ($[M]_0$ = 0.5 M) was added to a $CHCl_3$ solution of $[Rh(nbd)Cl]_2$ ($[M]_0/[Rh]$ = 50) and Et_3N ($[Rh]/[Et_3N]$ = 1/10) in a glass tube equipped with a three-way stopcock under dry nitrogen, and the solution was kept at 30 °C for 24 h. The reaction mixture was poured into a large amount of methanol to precipitate a polymer. The resulting polymer was separated by filtration and dried under reduced pressure.

Spectroscopic Data of the Polymers. Poly(1a). IR ($CHCl_3$): 3317, 3019, 1650, 1545, 1216, 740, 669 cm^{-1}. ^{1}H NMR ($CDCl_3$): δ 1.48−1.88 (C*H*$_3$), 4.20−4.54 (C═CC*H*$_2$), 4.54−5.20 (C*H*), 5.45−6.10 (C═C*H*), 6.30−9.10 (Ar*H*, N*H*).

Poly(1b). IR ($CHCl_3$): 3310, 1650, 1547, 1237, 741, 644 cm^{-1}. ^{1}H NMR ($CDCl_3$): δ 0.40−0.82 ($CH_2CH_2CH_2CH_2CH_2CH_3$), 0.82−1.18 ($CH_2CH_2CH_2CH_2CH_2CH_3$), 1.18−1.40 ($CH_2CH_2CH_2CH_2CH_2CH_3$), 1.40−1.84 (C*H*$_3$), 2.38−2.80 ($CH_2CH_2CH_2CH_2CH_2CH_3$), 4.20−4.46 (C═CC*H*$_2$), 4.46−5.00 (C*H*), 5.40−5.80 (C═C*H*), 6.40−8.40 (Ar*H*, N*H*).

Poly(2a). IR ($CHCl_3$): 3296, 1649, 1541, 1214, 737, 689 cm^{-1}. ^{1}H NMR ($CDCl_3$): δ 2.90−3.44 ($CH_2C_6H_5$), 3.68−4.22 (C═CC*H*$_2$), 4.52−5.08 (C*H*), 5.80−6.14 (C═C*H*), 6.40−7.88 (Ar*H*), 7.88−8.20 (N*H*).

Poly(2b). IR ($CHCl_3$): 3296, 1656, 1542, 685 cm^{-1}. ^{1}H NMR ($CDCl_3$): δ 0.60−0.96 ($CH_2CH_2CH_2CH_2CH_2CH_3$), 1.06−1.38 ($CH_2CH_2CH_2CH_2CH_2CH_3$), 1.38−1.68 ($CH_2CH_2CH_2CH_2CH_2CH_3$), 2.30−2.70 ($CH_2CH_2CH_2CH_2CH_2CH_3$), 2.72−3.40 ($CH_2C_6H_5$), 3.80−4.32 (C═CC*H*$_2$), 4.66−5.00 (C*H*), 5.30−6.10 (C═C*H*), 6.40−7.90 (Ar*H*), 7.90−8.58 (N*H*).

Poly(3). IR ($CHCl_3$): 3301, 1661, 1531, 1218, 743, 668 cm^{-1}. ^{1}H NMR ($CDCl_3$): δ 4.60−5.10 (C*H*), 5.20−6.18 (C═C*H*), 6.40−8.50 (Ar*H*, N*H*).

Poly(4). IR ($CHCl_3$): 3422, 3308, 3019, 2929, 2857, 1648, 1540, 1218, 727, 668 cm^{-1}. ^{1}H NMR ($CDCl_3$): δ 0.80−0.87 ($CH_2CH_2CH_2CH_2CH_2CH_2CH_3$),1.18−1.50($CH_2CH_2CH_2CH_2CH_2CH_2CH_3$), 1.55−1.60 (C*H*$_3$), 1.60−2.00 ($CH_2CH_2CH_2CH_2CH_2CH_2CH_3$) 3.60−4.12 ($CH_2CH_2CH_2CH_2CH_2CH_2CH_2CH_3$), 4.15−4.90 (C═CC*H*$_2$, C*H*), 5.50−5.80 (C═C*H*), 6.00−8.00 (Ar*H*, N*H*).

Photoisomerization. A sample solution was irradiated in a quartz glass tube with a 400 W high-pressure mercury lamp (Fuji Glass Work HB-400). To irradiate at 300 nm < λ < 400 nm, Pyrex glass and Toshiba D33S filters were used. To irradiate at 400 nm < λ < 500 nm, Pyrex glass and Toshiba L42 filters were used. The distance between the sample and lamp was set at 20 cm.

Simulation of CD Spectra. First, a 18-mer of **1b** was constructed and energy-minimized by the use of molecular mechanics with MMFF94 forcefield[19] on Wavefunction, Spartan '04 Windows to yield a stable helical conformer with all *trans* conformations of azobenzene side chains. Recently, ZINDO/S-based simulations of CD spectra were shown to reproduce experimental CD spectra.[20] Thus, the CD spectrum of the helical polymer was predicted essentially according to ref 20a, based on the time-dependent SCF (ZINDO/S) method in Gaussian 03.[21] Since the total atomic number was beyond our computational capability, the optimized structure was downsized as follows. All hexyl side chains were changed to methyl groups. Furthermore, the molecule was divided into two at the center; each helical fragment having nine azophenoxy units (which is shown in Figure 2) was subjected to the Gaussian 03 computation to predict the transition-state properties.[22] Under a CI number of 200 × 200, the low-energy transition states of 200 were predicted with each oscillator strength (f_{vel}) and rotatory strength (R_{vel}) in velocity form. To produce CD spectra, the R_{vel}−wavelength data were treated with a wavelength-based Gaussian function with a half of 1/e-bandwidth (tentatively, 10 nm).[20a,d,e,23] Here, a similar function was applied to the f_{vel}−wavelength data to estimate the corresponding absorption profile.

Results and Discussion

Monomer Synthesis. Azobenzene-containing novel monomers **1a**−**3** were synthesized according to the routes illustrated in Scheme 2. We first tried to synthesize **1a** and **1b** via (*S*)-2-hydroxy-*N*-propargylpropionamide, which was synthesized by the reaction of L-(+)-lactic acid with propargylamine, but failed to isolate (*S*)-2-hydroxy-*N*-propargylpropionamide either by column chromatography or distillation due to its high polarity and boiling point. We therefore synthesized the methyl esters of (*R*)-2-(4-phenylazophenoxy)propionic and (*R*)-2-[4-(4-hexylphenylazo)phenoxy]propionic acids first by the Mitsunobu

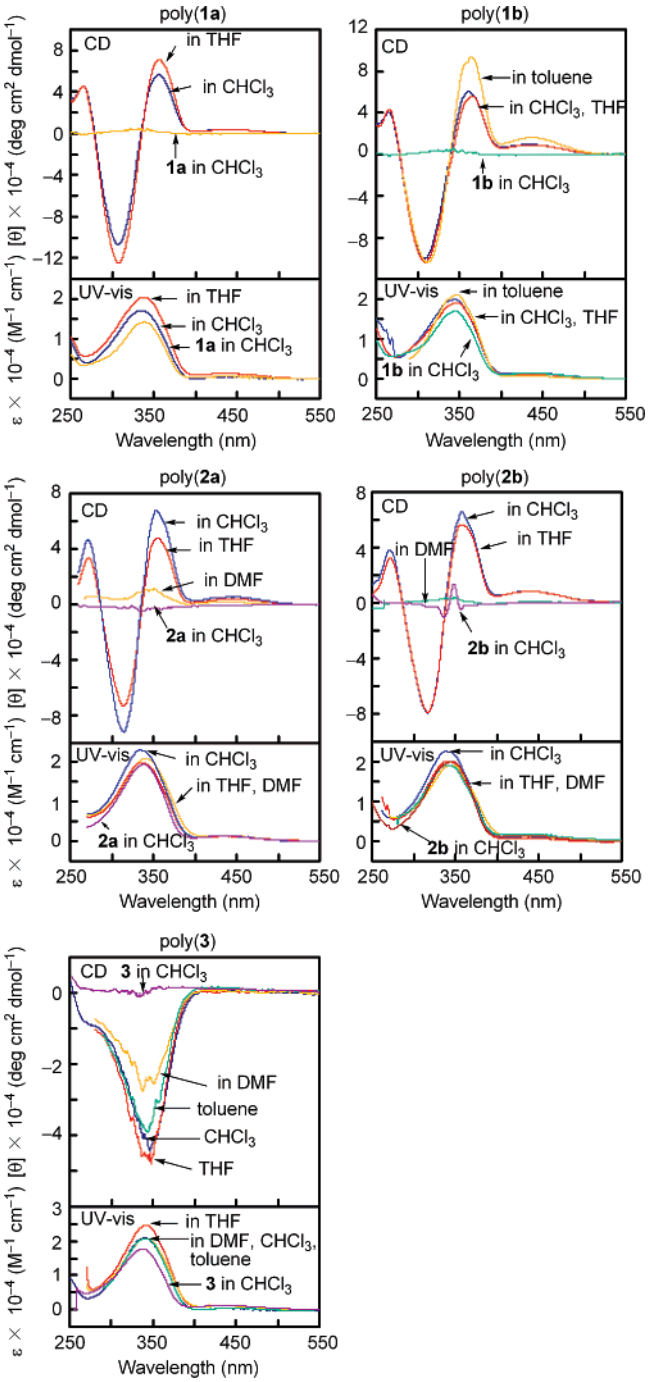

Figure 1. CD and UV−vis spectra of poly(**1a**)−poly(**3**) and the corresponding monomers measured in $CHCl_3$, THF, toluene, and DMF at room temperature (c = 0.100 mM).

reaction of methyl (*S*)-(−)-lactate with both 4-hydroxyazobenzene and 4-(4-hexylphenylazo)phenol, hydrolyzed them to obtain the corresponding carboxylic acids, and then condensed the acids with propargylamine, respectively.

On the contrary, since we could successfully isolate (*R*)-2-hydroxy-3-phenyl-*N*-propargylpropionamide and (*R*)-2-hydroxy-2-phenyl-*N*-propargylacetamide by column chromatography, we synthesized monomers **2a**−**3** by the Mitsunobu reaction of the *N*-propargylamides with hydroxyazobenzene derivatives using diisopropyl azodicarboxylate and triphenylphosphine.[24] In the present study, inversion of the chiral center during the Mitsunobu reaction was confirmed by X-ray structure analysis of a single crystal,[25] and the optical purity of the formed monomer was almost quantitative.[26]

Polymerization. The polymerization of **1a**−**3** was carried out with $[Rh(nbd)Cl]_2$-Et_3N as a catalyst in $CHCl_3$. The results of the polymerization are listed in Table 1. Polymers with moderate molecular weights (M_n = 6900−44 000) were obtained in 46−99% yields. The structures of the polymers were determined by IR and ^1H NMR spectroscopies. In the IR spectra of the polymers, the absorption peaks assignable to C≡C stretching vibration observed in the monomers disappeared, indicating that acetylene polymerization proceeded to give poly(**1a**)−poly(**3**) as illustrated in Scheme 1. We confirmed that poly(**1a**)−poly(**3**) took a *cis*-stereoregular structure, because they clearly exhibited a ^1H NMR signal around 6.0 ppm assignable to a *cis*-vinyl proton in the main chain, similarly to Rh-based poly(*N*-propargylamides) reported so far.[9] The optical rotations ($[\alpha]_D$) of the polymers measured in $CHCl_3$ were much larger than those of the corresponding monomers. It is suggested that the polymers form a helical structure with predominantly one-handed screw sense. All the polymers completely dissolved in $CHCl_3$ and THF, and partly or totally dissolved in toluene and DMF (Table S1). Introduction of hexyl group slightly increased the solubility as seen from the comparison between poly(**1a**) and poly(**1b**) and between poly(**2a**) and poly(**2b**).

Conformation of the Polymers in Solution. Figure 1 depicts the CD and UV−vis spectra of poly(**1a**)−poly(**3**) measured in $CHCl_3$, THF, toluene, and DMF at room temperature, along with the corresponding monomers. All the polymers and monomers displayed a strong UV−vis absorption band assignable to π−π* transition of *trans*-azobenzene at 340 nm in all the solvents. Poly(**1a**)−poly(**2b**) exhibited an intense split Cotton effect at this region in $CHCl_3$, THF, and toluene. This behavior is typical of exciton coupling by cooperative interaction between azobenzene chromophores in the side chains, which are arranged in a mutual chiral geometry of one-handed screw sense.[27] Judging from the positive first and negative second Cotton effects, the helical array of azobenzene moieties is considered to be right-handed.[28] This means that the main chain of the polymers also forms a helix with predominantly one-handed screw sense.

IR spectra of the monomers and polymers were measured in $CHCl_3$ (c = 50 mM) to check the presence of hydrogen bonds. The amide I and II absorption peaks of the monomers were observed at 1681−1685 and 1515−1521 cm^{-1}, respectively (Table S2). These peaks should be derived from the amide groups free from hydrogen bonding, because the concentration is low enough to prevent them from forming intermolecular hydrogen bonding. On the other hand, the amide I and II absorption peaks of the corresponding polymers were observed at 1649−1661 and 1531−1547 cm^{-1} at the same concentration, respectively. The wavenumbers of these IR bands were independent of the concentrations in the range from 1.0 to 50 mM. Consequently, it is concluded that hydrogen bonding is formed between the amide groups of the polymers intramolecularly.

To obtain further information, CD spectra were simulated for two possible helical conformers of 9-mers of **1b** (illustrated in the red and blue boxes of Figure 2) according to the procedure described in the experimental section. As shown in Figure 2, positive and negative CD signals appeared around 430−450 nm, whereas no significant f values were seen in the corresponding region. Since such CD signals were not experimentally observed, the effect of weak transitions (such as n → π*) seemed to be overestimated in the present simulation of CD spectra. The transition-state properties at 250−360 nm correspond to the main spectra experimentally observed at 250−380 nm. The CD

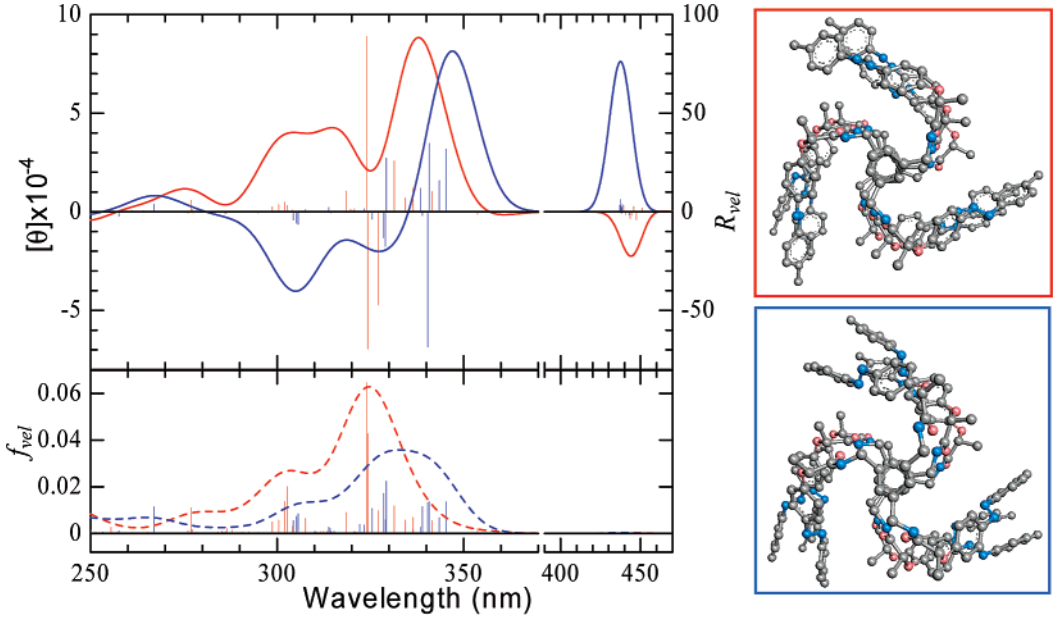

Figure 2. Simulated CD spectra of two 9-mers of **1b** (all hexyl groups were changed to methyl groups) with *trans*-azobenzene in helical conformations. [θ], R_{vel}, and f_{vel} are expressed per monomer unit. Red and blue lines correspond to the right figures.

Scheme 2. Synthesis of 1a−3

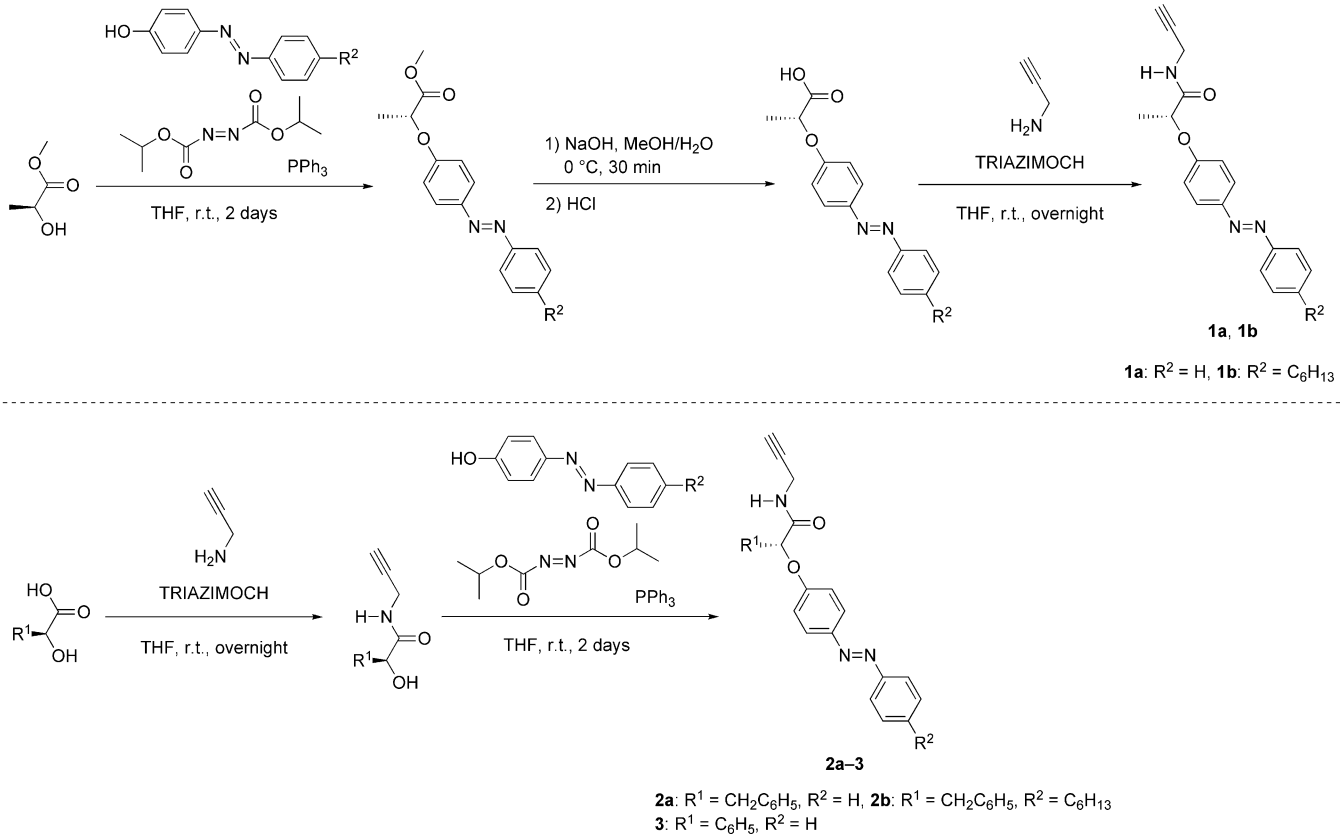

spectra simulated for the two helices yielded positive signals at 340−350 nm, followed by negative or weakly positive ones at 320−330 nm. This split or splitlike pattern supports the experimental CD spectra, thus originating from a clockwise twist of neighboring azobenzene pairs. The positive signals predicted at 265−280 nm should be essentially based on the π-conjugation in the backbone. Both patterns and signs at 320−330 and 265−280 nm based on the simulation well coincide with the experimental spectra. In contrast, the two conformations produce opposite CD signs at 295−310 nm, although the helical symmetries of the backbone are similar to each other. The CD signs should be addressed to relative orientations of azobenzene side chains. The experimental CD patterns suggest that the blue conformer is more likely than the red one, while both states will be populated in equilibrium. Further analysis might be required for comprehensive understanding of the CD pattern−structure relationship. However, it is noteworthy that such a helical conformation shown in Figure 2 is supported from the theoretical CD simulation at molecular orbital levels.

As shown in Figure 1, poly(**2a**) and poly(**2b**) exhibited no intense CD signal in DMF, in which it should be difficult to form intramolecular hydrogen bonds between the polymer

Table 1. Polymerization of 1a−3[a]

monomer	yield[b] (%)	M_n[c]	M_w/M_n[c]	viscosity index[d]	$[\alpha]_D$ (deg)[e]
1a	76	21 000	2.95	1.42	+468
1b	99	33 000	2.50	1.35	+603
2a	84	18 000	1.79	0.93	+402
2b	46	6900	2.40	1.15	+117
3	74	44 000	1.74	1.22	−710

[a] Polymerized with $[(nbd)RhCl]_2$-Et_3N in $CHCl_3$ at 30 °C for 24 h. $[M]_0 = 0.50$ M, $[Rh] = 5.0$ mM, $[Et_3N] = 10$ mM. [b] MeOH-insoluble part. [c] Estimated by GPC (eluent $CHCl_3$, PSt calibration). [d] Determined by GPC equipped with a viscometer detector (eluent THF). [e] Measured by polarimetry in $CHCl_3$ at room temperature ($c = 0.10$ g/dL).

molecules. It seems that the intramolecular hydrogen-bonding plays an important role for the polymers to form a helix. We could not observe apparent CD and UV−vis signals assignable to the polyacetylene main chain, presumably because of the smaller intensity than that of azobenzene moieties. The polyacetylene-based CD and UV−visible signals will be discussed later. It is noteworthy that poly(**3**) displayed completely different CD spectroscopic patterns from those of poly(**1a**)−poly(**2b**). Further, poly(**3**) also showed an intense CD signal in DMF. The way of helical array of azobenzene moieties of poly(**3**) should be largely different from the others. The phenyl group of poly(**3**) adjacent to the chiral center may cause this difference, but the concrete reason is unclear.

Temperature Dependence of the Polymer Conformation. Figure 3 depicts the CD and UV−vis spectra of poly(**1a**), poly(**2a**), and poly(**3**) measured in $CHCl_3$ at 0−50 °C. The CD and UV−vis spectra of poly(**1a**) changed little upon raising temperature from 0 to 50 °C. The helical structure of poly(**1a**) was stable against heating. On the other hand, the CD intensity of poly(**2a**) gradually decreased by raising temperature from 0 °C, and became 60% at 50 °C compared with the one at 0 °C. Commonly, reduction of CD intensities indicates the decrease of one-handedness and/or transformation of helix into random coil structure. Since there was no change of the UV−vis spectra of poly(**2a**) upon raising temperature, it is likely that the inversion of the helical sense took place in the present case. Surprisingly, the CD intensity of poly(**3**) did not decrease but increased by raising temperature, which means that the ratio of one-handed helicity increased. This phenomenon is completely opposite to the helical poly(*N*-propargylamides) reported so far, which diminish the CD intensity upon raising temperature.[12] At lower temperature, the phenyl group close to the main chain may disturb the polymer to take a regulated structure due to steric repulsion to some extent. At higher temperature, steric strain around the phenyl group may be released, allowing the polymer to take a regulated structure more efficiently. A change of the arrangement of the side chains also possibly causes the CD spectral change of poly(**3**) upon heating.

Photoinduced Conformation Change. Figure 4 depicts the change of CD and UV−vis spectra of poly(**1a**), poly(**2a**), and poly(**3**) during the photoisomerization process. When the polymer solutions in $CHCl_3$ were irradiated in a quartz glass cell with a 400-W high-pressure mercury lamp through a Pyrex glass filter to exclude the light of the wavelength below 300 nm and above 400 nm, the UV−vis absorption at 340 nm decreased the intensity accompanying blue shift to 320 nm with irradiation time, and the intensity stopped decreasing after 8−15 min. This means that the *trans*-azobenzene moieties isomerized into *cis* form upon irradiation of UV-light with 300−400 nm. The degrees of decrease ranged from 41 to 46%. The absorption attributable to n−π* transition of *cis*-azobenzene around 440 nm increased slightly during UV irradiation. The split CD signals of poly(**1a**) and poly(**2a**) centered at 340 nm, attributable to helical azobenzene array, decreased the intensities upon irradiation of UV-light. This result indicates that the *trans*-azobenzene moieties decreased the helicity in conjunction with the isomerization into the *cis* form. It should be noted that the λ_{max} of the UV−vis spectra became the same wavelength (310 nm) as the negatively signed CD signals after UV irradiation. It is likely that this absorption comes from the conjugated polyacetylene backbone taking a helical structure. This assumption reasonably explains the larger intensity of the negative second Cotton effect than that of the positive first one before UV irradiation.

To obtain information on the CD and UV−vis signals based on the polyacetylene backbone, we synthesized poly(**4**) carrying no azobenzene (Chart 1),[29] an analogous polymer to poly(**1a**) and poly(**1b**). Poly(**4**) exhibited an intense bisignate CD pattern, a minus first signal at 310 nm and a plus second one at 270 nm as depicted in Figure 5. No CD signal of monomer **4** indicates that the bisignate CD pattern of poly(**4**) comes from the helical polyacetylene backbone of poly(**4**). The broad UV−vis absorption corresponding to the band edge of the CD signal also supports this conclusion. Judging from the structural resemblance between poly(**4**) and the present azobenzene-carrying polymers, the CD signal of poly(**1a**)−poly(**2b**) at 310 nm is regarded as the sum of the minus second Cotton effect based on the exciton chirality of helical azobenzene arrays and the minus first one based on the helical polyacetylene backbone as illustrated in Figure 6. The observed CD signals of Figure 6a, consisting of a plus the first Cotton signal (I^+) at 360 nm, minus a second one (II^-) at 310 nm, and plus a third one (III^+) at 260 nm, result from the CD signals based on the helical azobenzene array (b) and helical polyacetylene main chain (c). In the case of poly(**4**), there was no evidence of the formation of helical arrays of the benzene units; it exhibited no CD pattern based on the exciton chirality at the wavelength region around 280 nm, where benzene chromophore of **4** showed UV−vis absorption.

The helices of poly(*N*-propargylamides) are categorized into two patterns; one is the helix showing CD and UV−vis signals around 390 nm, and the other is the one showing them around 300 nm.[14,30] It is considered that the hydrogen bonding forms between the amide units at *n*th and $(n + 2)$th units in the former, and between the units at *n*th and $(n + 3)$th units in the latter. Poly(*N*-propargylcarbamates)[31] and poly(*N*-butynylamides)[32] belong to the latter case. The difference of the wavelength between them reflects the difference of conjugation length of the polyacetylene backbone. Namely, monosubstituted helical polyacetylene backbone with a longer helical pitch conjugates more than the one with a shorter helical pitch.[33] In the present study, we simulated the molecular models of poly(**1b**) to find that it takes a tight helix preferably to a loose one,[34] which agreed with the result obtained from the CD and UV−vis spectroscopic studies.

We further examined the helical structures of the polymers by ^1H NMR spectroscopy using the differential NOE technique, wherein poly(**2b**) and poly[(*S*)-*N*-propargyl-2-methyloctanamide] [poly(**5**), Chart 2][35] were subjected to measurement. When the vinyl proton on the main chain (indicated with a blue circle in Figure 7) was irradiated, the signal of amide methylene protons ($-CH_2NHCO-$, indicated with a white circle in Figure 7) increased the intensity due to NOE effect, and the value of poly(**2b**) (24%) was larger than that of poly(**5**) (18%). As described above, poly(**2b**) seems to take a tightly twisted conformation corresponding to the top one of Figure 7, and poly-

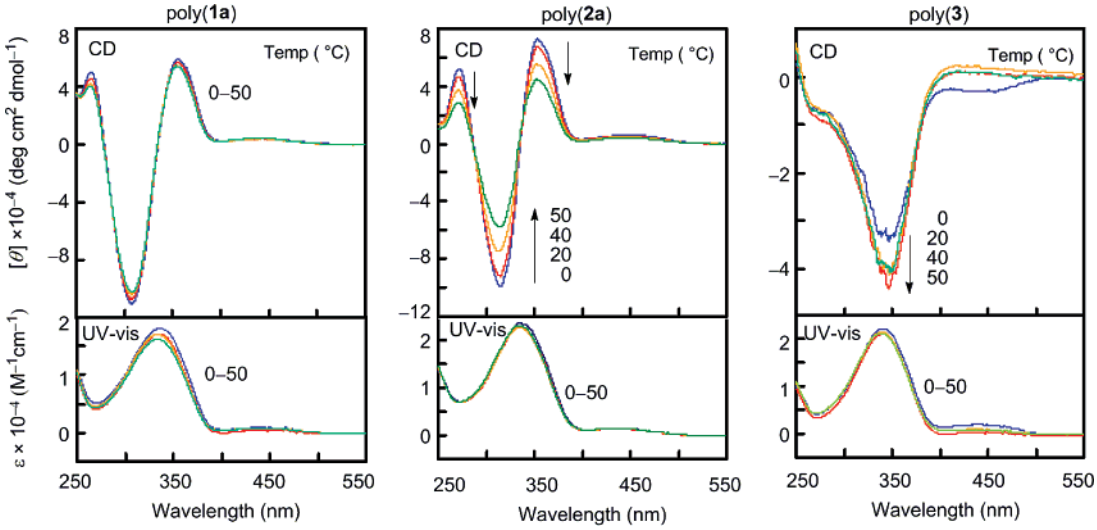

Figure 3. Changes in CD spectra of poly(**1a**), poly(**2a**), and poly(**3**) measured in $CHCl_3$ at 0−50 °C (c = 0.100 mM).

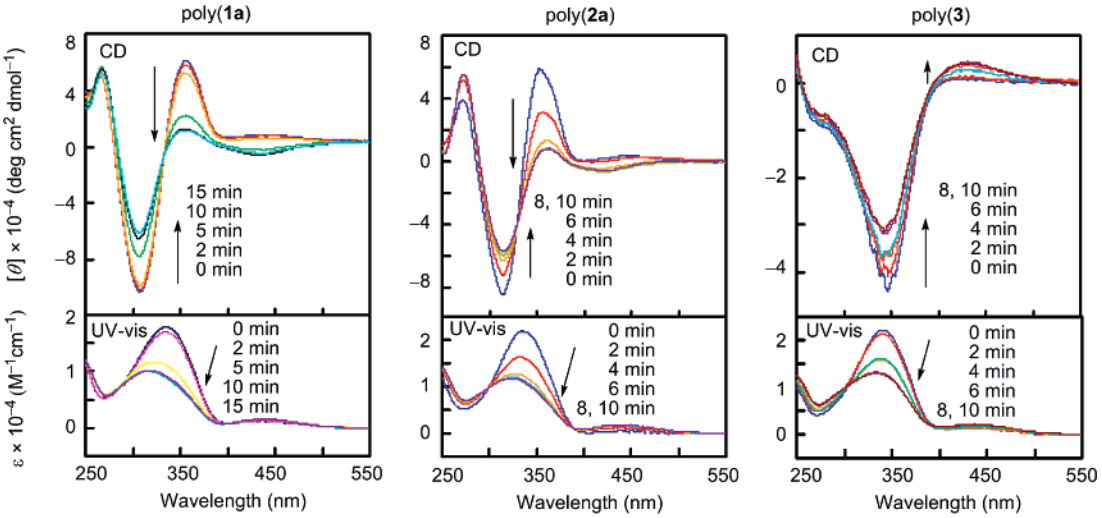

Figure 4. Variation of the CD and UV−vis spectra of poly(**1a**), poly(**2a**), and poly(**3**) with irradiation at 300 nm < λ < 400 nm in $CHCl_3$ at room temperature (c = 0.100 mM).

Chart 1

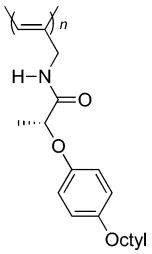

poly(**4**)

(**5**) does a loose one corresponding to the bottom one of the figure, because poly(**5**) exhibits CD and UV−vis signals around 400 nm,[35] a much longer wavelength region compared with that for poly(**2b**). In the case of a tight helix (Figure 7, top), one vinyl proton has two neighboring amide methylene protons: one is positioned in the same unit, and the other is positioned three units away; the interatomic distances between the vinyl and methylene protons are 2.31 and 2.19 Å (average 2.25 Å). All the other amide methylene protons are located more than 3.2 Å away from the vinyl proton, whose NOE effect should be very small. Meanwhile, in the case of the loose helix (Figure 7, bottom), one vinyl proton has two neighboring amide methylene protons; one is positioned in the same unit, and the other is positioned two units away. The interatomic distances are 2.29 and 2.38 Å (average 2.34 Å). Therefore, the larger NOE effect of poly(**2b**) than that of poly(**5**) is quite reasonable judging from their conformations.

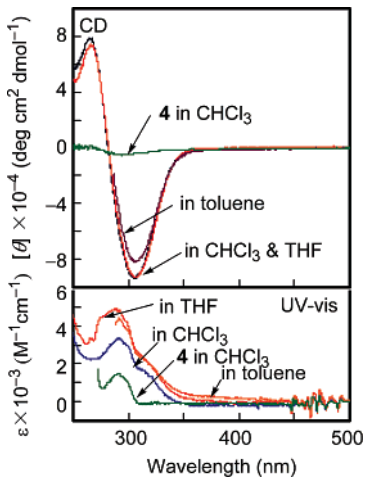

Figure 5. CD and UV−vis spectra of **4** and poly(**4**) measured in $CHCl_3$, THF, and toluene at room temperature (c = 0.100 mM).

Considering the fact that the UV−vis absorption and the minus CD signal at 310 nm did not disappear after UV

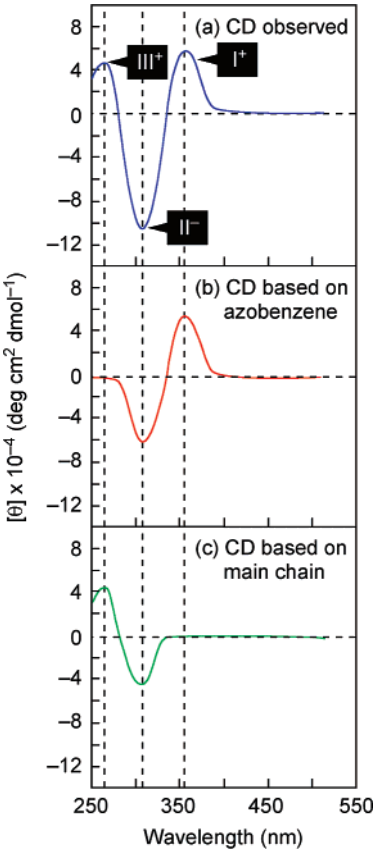

Figure 6. Assignment of the observed CD spectra of poly(**1a**)−poly(**2b**). The intensities of the signals are adjusted to the CD spectrum of poly(**1a**) measured in $CHCl_3$ depicted in Figure 1.

Chart 2

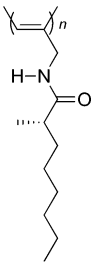

poly(**5**)

irradiation in spite of the disappearance of the plus CD signal at 370 nm, we can say that the polyacetylene backbone kept a helical structure with predominantly one-handed screw sense. In a similar fashion, the CD intensity of poly(**3**) at 340 nm decreased after UV irradiation to some extent, and leveled off at 72%. Consequently, the main chain also kept helicity after isomerization of *trans*-azobenzene into the *cis* form. The CD signal at 430 nm attributable to a n−π* transition of *cis*-azobenzene appeared instead of a decrease of the CD signal at 340 nm, suggesting the formation of chiral arrangement of *cis*-azobenzene moieties to some extent.[36]

We next examined visible-light irradiation (420 nm < λ) to achieve reisomerization from the *cis* form into a *trans* one (Figure 8). The UV−vis absorption at λ_{max} = 340 nm of poly(**1a**), poly(**2a**), and poly(**3**) recovered the original value almost quantitatively upon visible-light irradiation for 10 min. The isomerization efficiency of the azobenzene group of the polymer side chains was very high. Along with the recovery of the UV−vis absorption based on *cis*-azobenzene, the CD signal of poly(**1a**) and poly(**2a**) recovered to 62 and 67%, respectively,

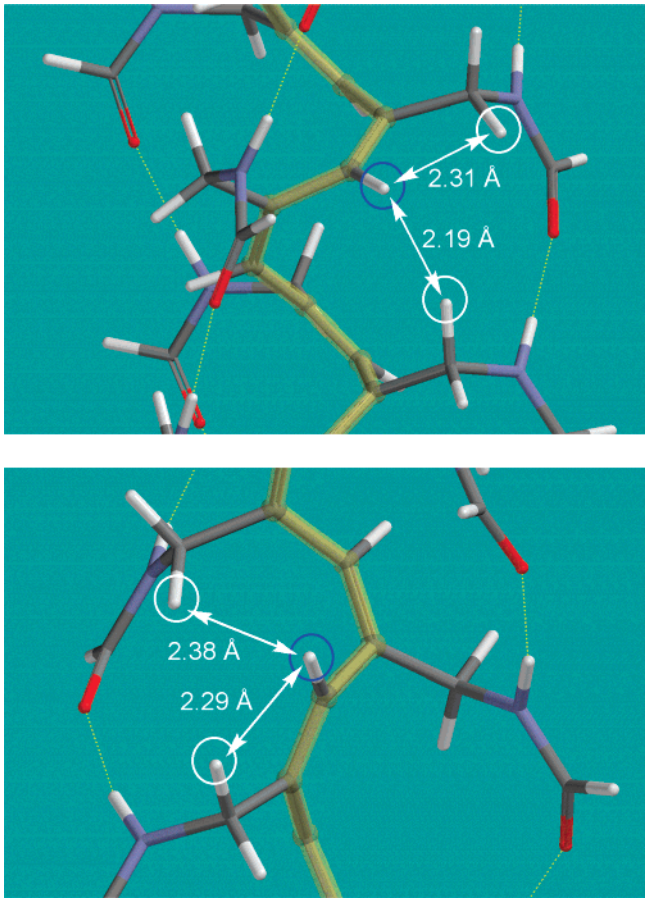

Figure 7. Conformations of a helical poly(*N*-propargylamide) forming hydrogen bonding between the amide groups at *n*th and (n + 3)th units representing the tight helix [e.g., poly(**2b**)] (top), and *n*th and (n + 2)th units representing the loose helix [e.g., poly(**5**)] (bottom). Herein conformers of poly(*N*-propargylformamide) are illustrated for clarity. The central yellow line is the polyacetylene backbone, and green dotted lines represent hydrogen bonds. The dihedral angles at the single bonds in the main chain are constrained to be 75 (top) and 125° (bottom) based on the conformational study depicted in Figure S2. All the other geometries are fully optimized with MMFF94.

indicating that azobenzene chromophores in the side chains rearranged in a mutual chiral geometry of predominantly one-handed screw sense to a certain degree. On the contrary, the CD signal of poly(**3**) did not change at all. The behavior was quite different from those of poly(**1a**) and poly(**2a**). It is assumed that the steric repulsion around the phenyl group next to the chiral center disturbs the rearrangement of azobenzene moieties, which may be related to the unusual thermodriven CD spectroscopic change as depicted in Figure 2.

Polarized Optical Microscope Images. Figure 9 depicts the polarized optical microscope images of poly(**1b**) taken as a 1,1,2,2-tetrachloroethane solution, and the sample after evaporation of the solvent. Poly(**1b**) exhibited a fingerprint texture in the solvent as shown in Figure 9a, indicating the formation of a cholesteric liquid crystal. The pitch of the texture pattern was 5.0 μm. Poly(**1b**) also showed similar fingerprint textures in $CHCl_3$, toluene, and THF, in which it formed a helix with predominantly one-handed screw sense as confirmed in Figure 1. On the other hand, poly(**1b**) exhibited no texture based on a liquid crystal in DMF, in which it took random coil structure. It is considered that the helical structure is essential for the polymer to form a liquid crystal.[37] It should be noted that this is the first observation of liquid crystalline property of a poly(*N*-propargylamide).

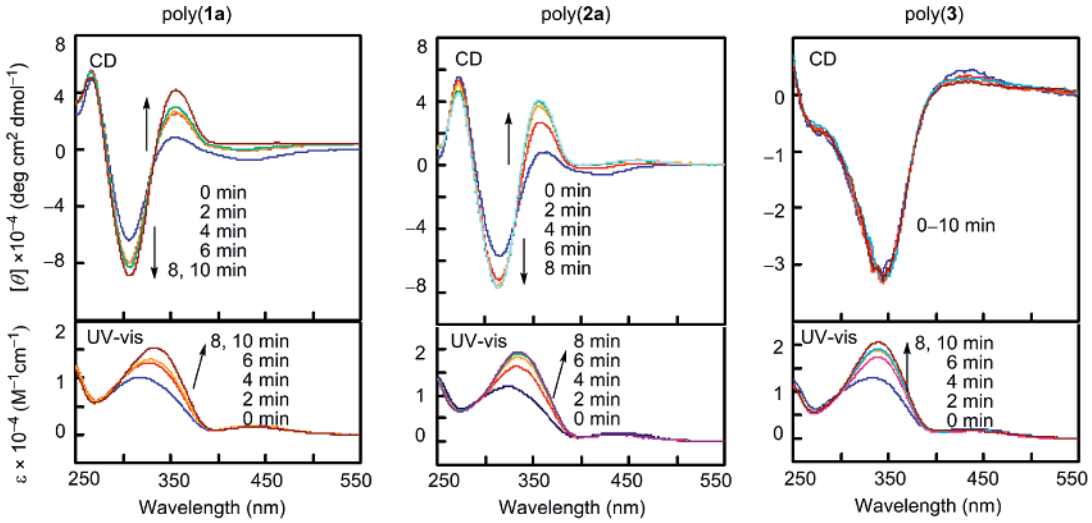

Figure 8. Variation of the CD and UV−vis spectra of poly(**1a**), poly(**2a**), and poly(**3**) with irradiation at 420 nm < λ in $CHCl_3$, after irradiation at 300 nm < λ < 400 nm at room temperature for 15 min (c = 0.100 mM).

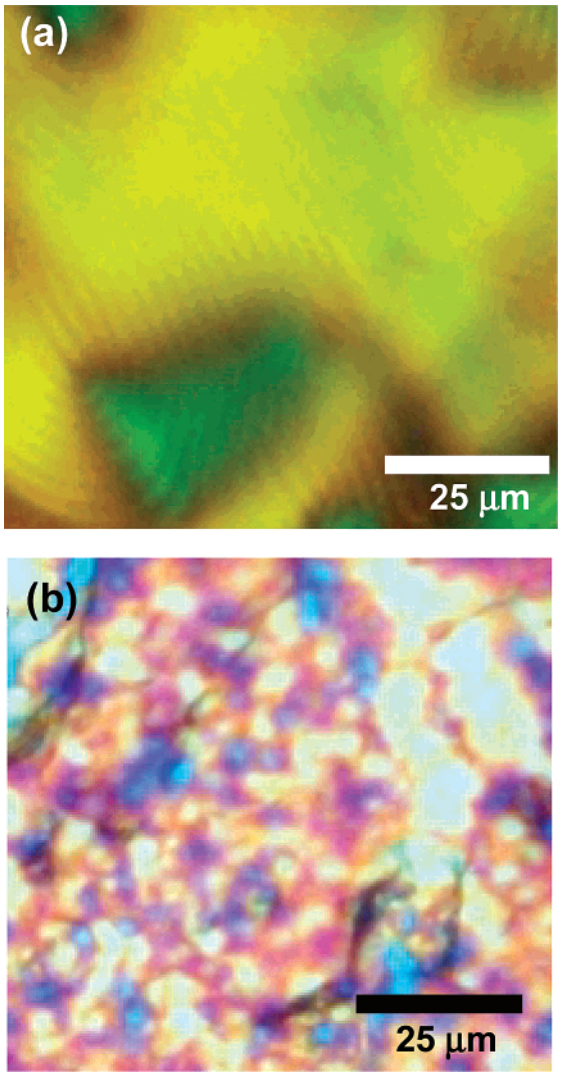

Figure 9. Polarized optical microscope images of poly(**1b**) captured (a) in 1,1,2,2-tetrachloroethane solution (15 wt %) and (b) after evaporation measured at room temperature.

Meanwhile, poly(**1a**), and poly(**2a**)−poly(**3**) did not exhibit such obvious fingerprint textures under the same conditions. Judging from the enough large viscosity indices in the Mark−Houwink−Sakurada equation of poly(**1a**)−poly(**3**) (0.93−1.42) as listed in Table 1, all the polymers are considered to take a stiff-rod conformation. Consequently, it seems that interchain interaction between long alkyl side chains as well as stiffness of the main chain based on one-handed helicity are also necessary for the present polymers to induce cholesteric liquid crystalline state. It is not clear why poly(**2b**) also carrying long alkyl side chains did not form a lyotropic liquid crystal. The more bulky benzyl group at the chiral center of poly(**2b**) may be unfavorable for polymer molecules to arrange regularly compared with the methyl group of poly(**1b**). Upon evaporation of the solvent, the fingerprint texture of poly(**1b**) turned into a different pattern as shown in Figure 8b, indicating the occurrence of phase change of the hierarchiral structure. Furthermore, we also tried to examine the change of liquid crystalline phase of poly(**1b**) with the isomerization of the azobenzne moieties upon UV-light irradiation, but could not get a convincing result, presumably due to the high concentration of the polymer (15 wt %) compared to the one in the CD and UV−vis spectroscopic experiment.

Conclusions

In this article, we have demonstrated the synthesis of chiral poly(*N*-propargylamides) [poly(**1a**)−poly(**3**)] carrying azobenzene in the side chains by the polymerization of the corresponding monomers using $[(nbd)RhCl]_2$-Et_3N as a catalyst. CD and UV−vis spectroscopic studies revealed that the polymers took predominantly one-handed helical structures in THF, $CHCl_3$ and toluene stabilized by hydrogen bonding between the amide groups at the side chains. The azobenzene chromophores in the side chains of poly(**1a**)−poly(**2b**) arranged in a mutual chiral geometry of predominantly one-handed screw sense. The *trans*-azobenzene of the polymer side chain isomerized into *cis* form upon UV irradiation, keeping the helicity of the polyacetylene backbone. The *cis*-azobenzene reisomerized into *trans*-form upon visible-light irradiation, accompanying the recovery of a helical array of azobenzene moieties in the cases of poly(**1a**) and poly(**2a**). It was concluded that the azobenzene moieties reversibly isomerized between *cis* and *trans* forms upon UV- and visible-light irradiation, and the formation of helical array was also reversible, while the isomerization of azobenzene did not affect the helical polyacetylene backbone. Although many examples of chirotopical switching based on the conformational

change of helical polymer main chain are reported, switching of helical orientation of the side chains keeping the helical conformation of the main chain intact is very rare.[38] Poly(**1b**) exhibited lyotropic liquid crystalline property, where the stiffness of the helical polymer backbone and the long alkyl chains were of key importance for the formation of cholesteric liquid crystalline state.

Acknowledgment. This research was partly supported by a Grant-in-Aid for Science Research in a Priority Area "Super-Hierarchical Structures (No. 446) " from the Ministry of Education, Culture, Sports, Science, and Technology, Japan. We appreciate Prof. Junji Watanabe at Tokyo Institute of Technology for helpful discussion about the liquid crystalline property of polymers, and Prof. Shigeru Yamago at Kyoto University for a suggestion about the NMR measurement.

Supporting Information Available: Solubility of poly(**1a**)−poly(**3**) (Table S1), IR spectroscopic data of **1a**−**3** and poly(**1a**)−poly(**3**) (Table S2), ORTEP drawing (Figure S1) and crystallographic information file (CIF) of **3′**, energy map of a helical 18-mer of **1b** with various torsion angles at the main chain (Figure S2), simulated CD spectra of 9-mers of **1b** with *cis*-azobenzene in helical conformations (Figure S3), and complete ref 21a. This material is available free of charge via the Internet at http://pubs.acs.org.

References and Notes

(1) (a) Natansohn, A.; Rochon, P. *Chem. Rev.* **2002**, *102*, 4139. (b) Griffiths, J. *Chem. Soc. Rev.* **1972**, *1*, 481.
(2) (a) Ramussen, P. H.; Ramanujam, P. S.; Hvilsted, S.; Berg, R. H. *J. Am. Chem. Soc.* **1999**, *121*, 4738. (b) Pieroni, O.; Houben, J. L.; Fissi, A.; Costantino, P.; Ciardelli, F. *J. Am. Chem. Soc.* **1980**, *102*, 5913.
(3) (a) Murk, R.; Zentel, R. *Macromolecules* **2002**, *35*, 185. (b) Mayer, S.; Zentel, R. *Macromol. Chem. Phys.* **1998**, *199*, 1675. (c) Mayer, S.; Maxein, G.; Zentel, R. *Macromolecules* **1998**, *31*, 8522. (d) Müller, M.; Zentel, R. *Macromolecules* **1996**, *29*, 1609. (e) Müller, M.; Zentel, R. *Macromolecules* **1994**, *27*, 4404.
(4) (a) Yu, Y.; Nakano, M.; Ikeda, T. *Nature (London)* **2003**, *425*, 145. (b) Tian, Y.; Watanabe, K.; Kong, X.; Abe, J.; Iyoda, T. *Macromolecules* **2002**, *35*, 3739. (c) Angiolini, L.; Bozio, R.; Giorgini, L.; Pedron, D.; Turco, G.; Dauru, A. *Chem.−Eur. J.* **2002**, *8*, 4241. (d) Andruzzi, L.; Altomare, A.; Ciardelli, F.; Solaro, R. *Macromolecules* **1999**, *32*, 448. (e) Angiolini, L.; Caretti, D.; Giorgini, L.; Salatelli, E.; Altomare, A.; Carlini, C.; Salaro, R. *Polymer* **1998**, *39*, 6621.
(5) Fujiki, M. *J. Am. Chem. Soc.* **2000**, *22*, 3336.
(6) Hida, N.; Takei, F.; Onitsuka, K.; Shiga, K.; Asaoka, S.; Iyoda, T.; Takahashi, S. *Angew. Chem., Int. Ed.* **2003**, *42*, 4349.
(7) Kosaka, N.; Oda, T.; Hiyama, T.; Nozaki, K. *Macromolecules* **2004**, *37*, 3159.
(8) (a) Kumar, G. S.; Neckers, D. C. *Chem. Rev.* **1989**, *89*, 1915. (b) Xie, S.; Natansohn, A.; Rochon, P. *Chem. Mater.* **1993**, *5*, 403.
(9) (a) Masuda, T.; Sanda, F.; Shiotsuki, M. Polymerization of Acetylenes. In *Comprehensive Organometallic Chemistry III*; Elsevier: Oxford, U.K., 2006; Vol. 11, Chapter 18. (b) Aoki, T.; Kaneko, T.; Teraguchi, M. *Polymer* **2006**, *47*, 4867. (c) Lam, J. W. Y.; Tang, B. Z. *Acc. Chem. Res.* **2005**, *38*, 745. (d) Masuda, T.; Sanda, F. Polymerization of Substituted Acetylenes. In *Handbook of Metathesis*; Grubbs, R. H., Ed.; Wiley-VCH: Weinheim, Germany, 2003; Vol. 3, Chapter 11.
(10) (a) Tabata, M.; Sone, T.; Sadahiro, Y. *Macromol. Chem. Phys.* **1999**, *200*, 265. (b) Kishimoto,Y.; Itou, M.; Miyatake, Y.; Ikariya, T.; Noyori, R. *Macromolecules* **1995**, *28*, 6662.
(11) (a) Yashima, E.; Huang, S.; Matsushima, T.; Okamoto, Y. *Macromolecules* **1995**, *28*, 4184. (b) Aoki, T.; Kokai, K.; Shinohara, E.; Oikawa, E. *Chem. Lett.* **1993**, *22*, 2009. (c) Ciardelli, F.; Lanzillo, S.; Pieroni, O. *Macromolecules* **1974**, *7*, 174.
(12) (a) Tabei, J.; Shiotsuki, M.; Sanda, F.; Masuda, T. *Macromolecules* **2005**, *38*, 5860. (b) Tabei, J.; Nomura, R.; Sanda, F.; Masuda, T. *Macromolecules* **2003**, *36*, 8603. (c) Nomura, R.; Tabei, J.; Nishiura, S.; Masuda, T. *Macromolecules* **2003**, *36*, 561. (d) Tabei, J.; Nomura, R.; Masuda, T. *Macromolecules* **2002**, *35*, 5405. (e) Nomura, R.; Tabei, J.; Masuda, T. *Macromolecules* **2002**, *35*, 2955. (f) Nomura, R.; Tabei, J.; Masuda, T. *J. Am. Chem. Soc.* **2001**, *123*, 8430.
(13) (a) Sanda, F.; Nishiura, S.; Shiotsuki, M.; Masuda, T. *Macromolecules* **2005**, *38*, 3075. (b) Nomura, R.; Nishiura, S.; Tabei, J.; Sanda, F.; Masuda, T. *Macromolecules* **2003**, *36*, 5076.
(14) Sanda, F.; Araki, H.; Masuda, T. *Macromolecules* **2005**, *38*, 10605.
(15) (a) Zhao, H.; Sanda, F.; Masuda, T. *Polymer* **2006**, *47*, 2596. (b) Sanda, F.; Teraura, T.; Masuda, T. *J. Polym. Soc., Part A: Polym. Chem.* **2004**, *42*, 4641.
(16) Kolasa, T.; Miller, M. J. *J. Org. Chem.* **1987**, *52*, 4978.
(17) Song, X.; Perlstein, J.; Whitten, D. G. *J. Am. Chem. Soc.* **1997**, *119*, 9144.
(18) Schrock, R. R.; Osborn, J. A. *J. Am. Chem. Soc.* **1971**, *93*, 2397.
(19) Halgren, T. A. *J. Comput. Chem.* **1996**, *17*, 490.
(20) (a) Komori, H.; Inai, Y. *J. Phys. Chem. A* **2006**, *110*, 9099. For the ZINDO/S method, see: (b) Zerner, M. C.; Loew, G. H.; Kirchner, R. F.; Mueller-Westerhoff, U. T. *J. Am. Chem. Soc.* **1980**, *102*, 589. (c) Ridley, J. E.; Zerner, M. C. *Theo. Chim. Acta* **1973**, *32*, 111. For the ZINDO-based simulation of CD spectra, see also: (d) Telfer, S. G.; Tajima, N.; Kuroda, R. *J. Am. Chem. Soc.* **2004**, *126*, 1408. (e) Ankai, E.; Sakakibara, K.; Uchida, S.; Uchida, Y.; Yokoyama, Y.; Yokoyama, Y. *Bull. Chem. Soc. Jpn.* **2001**, *74*, 1101.
(21) (a) Frisch, M. J.; et al. Gaussian 03, Revision C.02. Gaussian, Inc., Wallingford CT, 2004. (b) For the methods and full references in Gaussian 03, see: The Official Gaussian Website (http://www.gaussian.com).
(22) For the molecular modeling software, see: (a) Thompson, M. A. *ArgusLab 4.0*; Planaria Software LLC: Seattle, WA, 2004 (http://www.arguslab.com). For conversion of molecular data type, see also: (b) Senda, N. *Winmostar* (http://winmostar.com/); *Idemitsu Tech. Rep.* **2006**, *49*, 106.
(23) Harada, N.; Nakanishi, K. *Circular Dichroic Spectroscopy. Exciton Coupling in Organic Stereochemistry*; University Science Books: Mill Valley, CA, 1983.
(24) Mitsunobu, O. *Synthesis* **1981**, 1.
(25) See the Supporting Information (Figure S1).
(26) The enantiomeric excess of **1a** was 96%, which was determined by chiral HPLC equipped with a DAICEL CHIRALPAK IA, eluent hexane/2-propanol/ethyl acetate = 90/5/1 (volume ratio), comparing the chromatogram of **1a** with that of the racemic counterpart prepared from DL-lactic acid.
(27) Angiolini, L.; Caretti, D.; Carlini, C.; Salatelli, E. *Macromol. Chem. Phys.* **1995**, *196*, 2737.
(28) *Circular Dichroism: Principles and Applications. 2nd ed, Chapter 12*, Beroya, N.; Nakanishi, K.; Woody, R. W. Eds. Wiley-VCH (New York), 2000.
(29) Poly(**4**) was obtained by the polymerization of the corresponding monomer **4** under the conditions same as those in Table 1. Yield: 96%, M_n = 100 000, M_w/M_n = 2.57, and $[\alpha]_D$ = +402 deg (c = 0.10 g/dL in $CHCl_3$).
(30) (a) Sanda, F.; Terada, K.; Masuda, T. *Macromolecules* **2005**, *38*, 8149. (b) Sanda, F.; Araki, H.; Masuda, T. *Macromolecules* **2004**, *37*, 8510.
(31) (a) Sanda, F.; Nishiura, S.; Shiotsuki, M.; Masuda, T. *Macromolecules* **2005**, *38*, 3075. (b) Nomura, R.; Nishiura, S.; Tabei, J.; Sanda, F.; Masuda, T. *Macromolecules* **2003**, *36*, 5076.
(32) (a) Sanda, F.; Tabei, J.; Shiotsuki, M.; Masuda, T. *Sci. Tech. Adv. Mater.* **2006**, *7*, 572. (b) Tabei, J.; Shiotsuki, M.; Sanda, F.; Masuda,T. *Macromolecules* **2005**, *38*, 5860.
(33) Percec, V.; Obata, M.; Rudick, J. G.; De, B. B.; Glodde, M.; Bera, T. K.; Magonov, S. N.; Balagurusamy, V. S. K.; Heiney, P. A. *J. Polym. Sci., Part A: Polym. Chem.* **2002**, *40*, 3509.
(34) See the Supporting Information (Figure S2).
(35) Poly(**5**) was obtained by the polymerization of the corresponding monomer under the conditions same as those in Table 1. Yield: 61%. M_n = 36 000, M_w/M_n = 2.27, and $[\alpha]_D$ = +1060 deg (c = 0.10 g/dL in $CHCl_3$). Synthesis of poly(**5**): see Tabei, J.; Nomura, R.; Shiotsuki, M.; Sanda, F.; Masuda, T. *Macromol. Chem. Phys.* **2005**, *206*, 323.
(36) Molecular modeling of poly(**1b**) possessing *cis*-azobenzene pendants revealed that the *cis*-azobenzene moieties tend to lose the regularity due to steric repulsion, differently from the case of *trans*-azobenzene. The regularity of *cis*-azobenzene arrays seems to be low compared to that of *trans*-azobenzene ones. The simulated CD spectra of poly(**1b**) with *cis*-azobenzene are depicted in Supporting Information (Figure S3), in which the minus CD signal based on the *cis*-azobenzene moieties around 450 nm is predicted.
(37) Poly(**1b**) showed a CD spectroscopic pattern in 1,1,2,2-tetrachloroethane similar to those observed in $CHCl_3$, THF, and toluene.
(38) Tang, H. Z.; Boyle, P. D.; Novak, B. M. *J. Am. Chem. Soc.* **2005**, *127*, 2136.

MA070917J